Propagation of uncertainties in the Skyrme energy-density-functional model

Y. Gao,[1] J. Dobaczewski,[1,2] M. Kortelainen,[1] J. Toivanen,[1] and D. Tarpanov[2,3]

[1]*Department of Physics, P.O. Box 35 (YFL), FI-40014 University of Jyväskylä, Finland*
[2]*Institute of Theoretical Physics, Faculty of Physics, University of Warsaw, ul. Hoża 69, PL-00-681 Warsaw, Poland*
[3]*Institute for Nuclear Research and Nuclear Energy, 1784 Sofia, Bulgaria*

(Dated: January 28, 2013)

Parameters of nuclear energy-density-functionals (EDFs) are always derived by an optimization to experimental data. For the minima of appropriately defined penalty functions, a statistical sensitivity analysis provides the uncertainties of the EDF parameters. To quantify theoretical errors of observables given by the model, we studied the propagation of uncertainties within the UNEDF0 Skyrme-EDF approach. We found that typically the standard errors rapidly increase towards neutron rich nuclei. This can be linked to large uncertainties of the isovector coupling constants of the currently used EDFs.

PACS numbers: 21.60.Jz, 21.10.Dr, 21.10.Gv, 21.10.Ft, 21.30.Fe

arXiv:1301.6151v1 [nucl-th] 25 Jan 2013

Introduction. The nuclear energy-density-functional (EDF) approach is the only microscopic method that can be applied throughout the entire nuclear chart. Owing to the existing and future radioactive-beam facilities, the experimentally known region of the nuclear landscape will be pushed towards more and more exotic systems. New experimental data on nuclei with a large neutron or proton excess will put predictions of the current and future EDF models to test. Therefore, it is important to assess the uncertainties and predictive power of models [1–4].

The nuclear EDF models can best be formulated in terms of effective theories, tailored to low-energy phenomena with high-energy effects taken into account through model parameter adjustments. Although a rigorous application of the effective-theory methodology [5] is not yet fully implemented, the aspect of systematic adjustments of model parameters to data is always a crucial element of the approach. Only very recently, such adjustments are accompanied with the full covariance error analysis [6–9].

The aim of the present work is to study how uncertainties in the model parameters propagate to observables calculated within the model. This appears to be the simplest and most fundamental method to assess the predictive power of the model. First, the model is characterized not only by the fit residuals, that is, deviations between measured and calculated observables, but also by propagated uncertainties, which carry the errors of model parameters over to calculated observables. In this way, even the data points that have been used for the parameter adjustments are characterized by the propagated uncertainties.

A properly balanced parameter adjustment should, in principle, lead to propagated uncertainties, which are comparable in magnitude to fit residuals. Second, extrapolations of the model to unmeasured data points, which is, in fact, one of the principal goals of formulating models, bear no meaning if they are not accompanied by their propagated uncertainties. Indeed, large propagated uncertainties simply mean that relatively small deviations of model parameters, within the bounds of the adjustment, strongly influence the predicted values. On the one hand, this may give us invaluable information on which parameters of the model are grossly undetermined, and on the other hand, this may indicate which observables, when measured, would have the strongest impact on decreasing the errors of parameters.

There is, of course, another important class of theoretical uncertainties, which is not directly accessible through the statistical analysis of parameters, and which is very difficult to estimate, namely, the one stemming from the definition and limitation of the model itself, see discussion in Refs. [1, 3, 4, 10]. However, the statistical analysis may also here give us interesting information. Indeed, in cases when the propagated uncertainties turn out to be significantly smaller than the fit residuals, one may suspect that the model lacks important physics and/or new terms in the Hamiltonian (functional) and extended parameter freedom. This is so, because we are then in the situation of model parameters well constrained by some data, but not describing some other data correctly. This can be contrasted with the situation of propagated uncertainties larger than the fit residuals, when one cannot tell whether the model is deficient or whether its parameters are underdetermined.

Method. A good measure of theoretical uncertainty is to calculate the statistical standard deviation of an observable, predicted by the model. In the present, work we used the Skyrme EDFs [11] within the Hartree-Fock-Bogoliubov (HFB) nuclear structure calculations. To determine the propagation of uncertainties from the model parameters to some observable, predicted by the model, one needs information about the standard deviations and correlations between the model parameters. Some of the recent Skyrme-EDF parameter optimizations have provided this information [6, 7, 9]. In this work, to determine the propagation of theoretical uncertainties, we have chosen to use the UNEDF0 parameterization of the Skyrme EDF [7].

The calculated statistical error of an observable is linked with the covariance matrix of the nuclear EDF model parameters. From the Taylor expansion, we can find that the square of statistical error reads,

$$\sigma^2(y) = \sum_{i,j=1}^{n} \mathrm{Cov}\left(x_i, x_j\right) \left[\frac{\partial y}{\partial x_i}\right] \left[\frac{\partial y}{\partial x_j}\right], \qquad (1)$$

where y is the calculated observable, x_i is the parameter of the EDF and $\mathrm{Cov}(x_i, x_j)$ is the covariance matrix between parameters x_i and x_j. In the present work we use the covariance matrix that was obtained from the sensitivity analysis of the UNEDF0 parameterization, see Tables VIII and X of Ref. [7]. Another use of the covariance matrix consists in calculating covariance ellipsoids between pairs of observables [3, 8] and analyzing correlations between observables [12, 13].

Calculation of the standard error (1) requires calculation of derivatives of observable y with respect to model parameters x_i. As the relations between parameters and observables can be complicated, to calculate the derivatives one has to use numerical methods. By definition, the derivative of a function f can be approximated simply by a finite difference, $f'(a) \approx G_0(h) = \left(f(a+h) - f(a-h)\right)/2h$. To improve the accuracy, we used the Richardson extrapolation method [14],

$$G_m(h) = \frac{4^m G_{m-1}(h/2) - G_{m-1}(h)}{4^m - 1}, \qquad (2)$$

with $m = 1, 2, \ldots$, which then satisfies, $f'(a) - G_m(h) = \mathcal{O}(h^{2(m+1)})$. Generally speaking, a larger m means improved accuracy on derivatives with an increased cost of computational time. In this work we extrapolate up to $m = 2$ as a balanced point.

Large values h may lead to inaccurate derivatives, whereas small values may suffer from rounding errors. In this paper, we checked that when h changes for any parameter between 0.001% and 0.1% of the parameter's value, the calculated errors of observables do not change much. Thus values of h fixed in this region were used.

The HFB calculations were carried out by using the computer code HOSPHE [15, 16], which solves the HFB equations in a spherical harmonic-oscillator basis. We have run it within exactly the same conditions as those defined for the optimization of UNEDF0. In particular, calculations were done in the space of 20 major oscillator shells and the Lipkin-Nogami procedure of Ref. [17] with the pairing cut-off window of $E_{\mathrm{cut}} = 60\,\mathrm{MeV}$ was used. We determined ground-state properties of all even-even semi-magic nuclei with $N = 20$, 28, 50, 82, and 126 and $Z = 20$, 28, 50, and 82 extending between the two-proton and two-neutron driplines.

For UNEDF0, some of the very neutron rich Ca, Sn, and Pb isotopes turn to be deformed, see, e.g., supplementary material of Ref. [4]. The same also holds for some semimagic isotonic chains at the very neutron-rich regime. Since the current calculations are done with a spherical HFB solver, the calculated uncertainties may lack deformation effects. *A priori*, one can expect that the standard errors determined in spherical and deformed nuclei should be similar, see also Ref. [18], although in the future this conjecture must be tested in more extensive calculations. The aim of this work is to quantify a typical magnitude of the standard error related to an observable, and thus assess the overall predictive power of the model.

Results. In Fig. 1, we present the calculated standard errors of binding energies of semi-magic nuclei. The upper panel shows the isotonic chains with magic neutron numbers of $N = 20$, 28, 50, 82, and 126 and the lower panel shows the Ca, Ni, Sn, and Pb isotopic chains. Within the experimentally known regions of nuclei, where also data points were used during the EDF optimization, standard error usually stays rather constant and is typically of the order of 1 MeV. Moving to the neutron rich regime, calculated standard error increases rather steadily. This is directly related to the fact that the isovector parameters of the EDF are not constrained as well as the isoscalar ones [3, 7]. With isotonic (isotopic) chains, the nuclei with small Z (large N) of Fig. 1 are the ones with most neutron excess, and therefore standard deviation is largest in these nuclei. The values reached there can be of the order of 10 MeV, which means that for the total binding energies, when approaching the neutron drip line the predictive power of the model is rather poor.

For the Pb and $N = 126$ nuclei we also show, as an illustration, the moduli of fit residuals with respect to experimental data [19]. We note immediately, that the propagated error of the binding energy of ^{208}Pb of 0.41 MeV is much smaller than the fit residual of 4.07 MeV. This clearly indicates that no refined fits can probably account for this experimental data point, because the fit parameters are already quite rigidly constrained by other data. This result points to a missing physics in the description of the ^{208}Pb mass, which is most probably related to a poor description of the ground-states collective correlations in doubly magic systems, see discussion in Refs. [20–22].

In Fig. 2, the standard errors of two-neutron ($S_{2\mathrm{n}}$) and two-proton ($S_{2\mathrm{p}}$) separation energies are shown. Similarly as for the binding energies, within the experimentally know region, these standard errors stay rather small, that is, in heavy nuclei below 0.5 MeV for $S_{2\mathrm{p}}$ and below 0.25 MeV for $S_{2\mathrm{n}}$. Then, they start to increase rapidly when the calculations are extrapolated to neutron-rich regime, especially after the doubly magic gaps are crossed. Owing to the cancellation of errors, even in very exotic nuclei, the standard errors of two-particle separation energies are much smaller than those of the binding energies. This nicely illustrates the robustness of the position of two-neutron driplines discussed in Ref. [4].

In Figs. 3 and 4, we plot the standard errors of neutron and proton rms radii, respectively. One can see that the uncertainties related to the proton rms radii are much

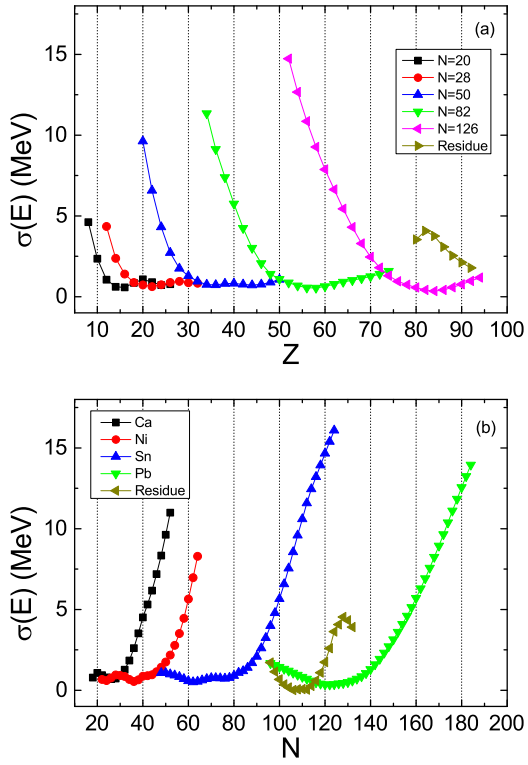

FIG. 1: (Color online) Standard errors of binding energies of semi-magic nuclei, calculated for (a) isotonic chains with magic neutron numbers and (b) isotopic chains with magic proton numbers. For the Pb and $N = 126$ nuclei, moduli of fit residuals with respect to experimental data [19] are also shown.

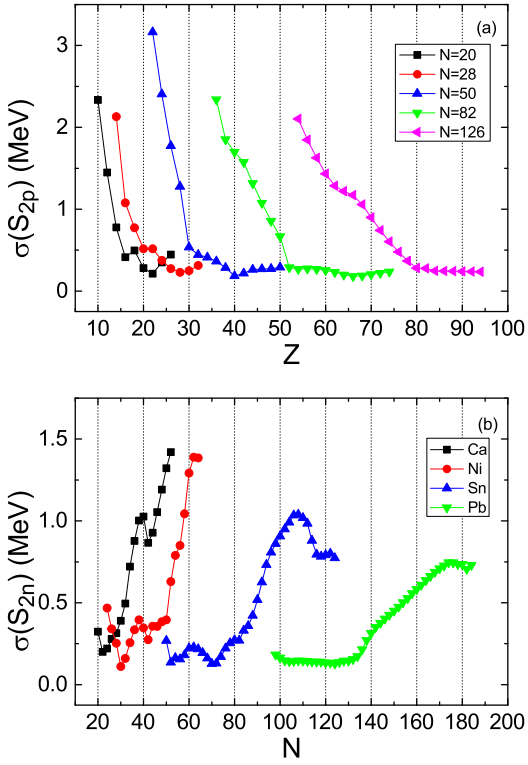

FIG. 2: (Color online) (a) Standard errors of two-proton separation energies S_{2p} for neutron semi-magic nuclei. (b) Standard errors of two-neutron separation energies S_{2n} for proton semi-magic nuclei.

smaller than those corresponding to neutron rms radii. This is directly related to the fact that in the optimization of the UNEDF0 parameter set, experimental input on the charge radii was used. For example, in ^{208}Pb we obtain $\sigma(R_n)$=0.062 fm and $\sigma(R_p)$=0.006 fm. The standard errors of neutron radii steadily increase towards the neutron drip line, again illustrating the large uncertainties in the isovector coupling constants of the functional. In heavy nuclei, the same is also true for protons, however, in light nuclei, the standard errors of proton radii also increase towards the proton drip line. This effect can be related to the weak binding of protons within a low Coulomb barrier. Uncertainties related to the proton and neutron rms radii are closely linked to the uncertainties of the neutron skin, see discussion in Ref. [18].

In Fig. 5, we present standard errors of the calculated mean-field (point-particle) proton and neutron densities in ^{208}Pb. Again we see that the standard errors of proton densities are significantly smaller than for neutrons, and that the neutron ones extend to much higher distances. The neutron density of Fig. 5d can be compared with the experimental weak-charge profile presented in Fig. 1 of Ref. [23], obtained from the PREX measurement at Jefferson Lab [24]. In the region of relative flat neutron density profile (that is, $R < 4$ fm) we find our standard errors to be 0.0035 fm^{-3} or less. In the same region, the incoherent sum of experimental and model errors [23] is roughly 0.0075 fm^{-3}. Even though the density profile of Fig. 5 is for a point-neutron density, folding it with a finite weak-charge distribution of neutrons, or including in the experimental estimate other small corrections, should not significantly change our result of propagated theoretical uncertainties being about twice smaller than the experimental ones.

Owing to the correlations between the model parameters, the standard errors calculated by using Eq. (1) can be strongly affected by the off-diagonal components of the covariance matrix. This is illustrated in Fig. 6, where various components of the sum contributing to squares of standard errors of the binding energy E (a), two-neutron separation energy S_{2n} (b), neutron rms radius R_n (c), and proton rms radius R_p (d) in ^{208}Pb are plotted. The order of the parameters used in Fig. 6 is the same as that used in the definition of the correlation matrix of UNEDF0, see Tables VIII and X of Ref. [7]. For the sake of completeness, these parameters are also listed in the caption of Fig. 6.

One sees from Fig. 6a that the standard error of the binding energy E results from a strong cancellation between large positive (> 500 MeV^2) diagonal contributions coming from a_{sym}^{NM} and L_{sym}^{NM} (parameters No. 3 and 4), and large negative (< -500 MeV^2) contributions coming

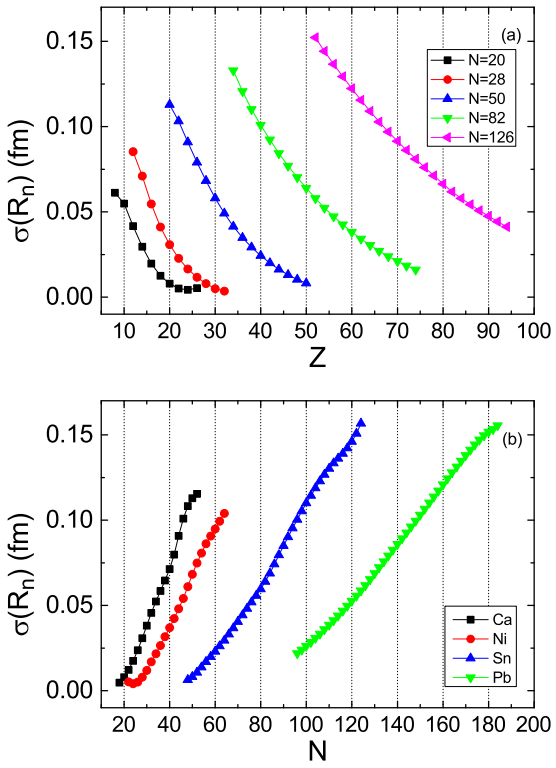

FIG. 3: (Color online) Same as in Fig. 1 but for the neutron rms radii.

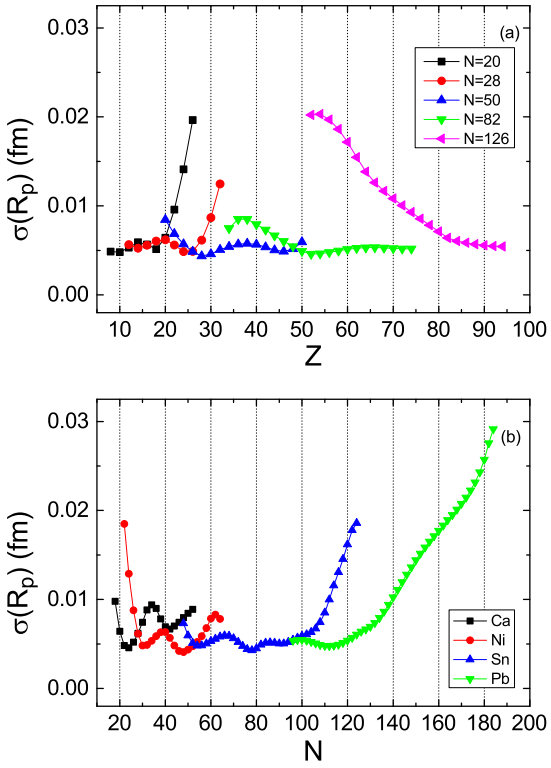

FIG. 4: (Color online) Same as in Fig. 1 but for the proton rms radii.

from the off-diagonal correlations between these two parameters. The remaining parameters of the functional give much smaller positive and negative contributions, bringing the final value to $\sigma^2(E)$=0.17 MeV^2. It is interesting to note that even in this well-bound nucleus, the largest uncertainties of the binding energy come from the poor symmetry-energy characterization of the functional.

The situation obtained for the standard error of S_{2n} (Fig. 6b) is quite similar. Although the value of $\sigma^2(S_{2n})$=0.02 MeV^2 is much smaller than that for the binding energy, it results form the cancellation of contributions coming form the above two parameters and $C_1^{\rho\Delta\rho}$ (parameters No. 6), which is the parameter characterizing the isovector surface properties of the functional. Again, the uncertainties in the isovector characterization of the functional dominate the standard error here.

The pattern obtained for the standard error of the neutron rms radius of $\sigma^2(R_n)$=3.8×10^{-3} fm^2 (Fig. 6c) is markedly different, with the single parameter L_{sym}^{NM} dominating the uncertainty of this variable, although again the isovector properties are to be blamed. Only for the proton rms radius (Fig. 6d), its fairly small standard error of $\sigma^2(R_p)$=4.1×10^{-5} fm^2 is given by contributions coming from a_{sym}^{NM} and isoscalar parameters ρ_c and $C_0^{\rho\Delta\rho}$.

Even though the single-particle (s.p.) energies are not strictly-speaking observables, they are nevertheless closely connected to observable levels of neighboring even-odd nuclei and to other nuclear properties like, e.g., deformations of open-shell systems. It is, therefore, interesting to discuss their standard errors and check how tightly their values are fixed by the adjustment of the functional to other observables, see also discussion in Ref. [6]. Since our calculations were performed with pairing correlations and Lipkin-Nogami corrections taken into account, we performed the analysis for the s.p. energies e_{HF} defined as the eigenstates of the mean-field part of the HFB Hamiltonian.

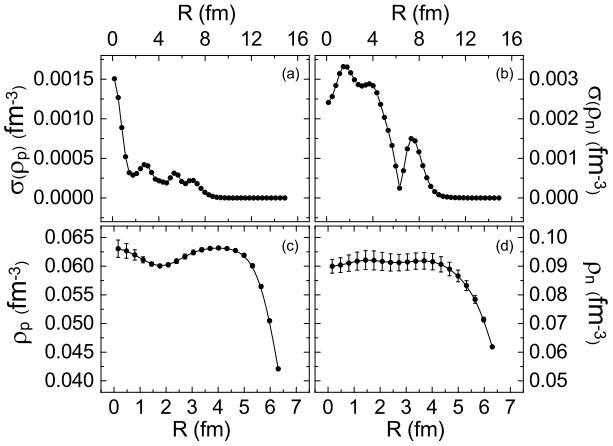

FIG. 5: Standard errors of densities in ^{208}Pb for (a) protons and (b) neutrons as functions of the radial variable R. Panels (c) and (d) show the proton and neutron densities, respectively, with the standard errors represented by error bars.

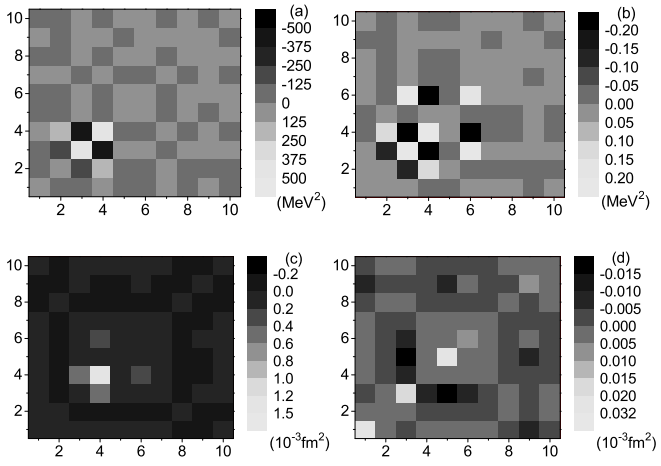

FIG. 6: Contributions of various components of the sum (1) to squares of standard errors of the binding energy E (a), two-neutron separation energy S_{2n} (b), neutron rms radius R_n (c), and proton rms radius R_p (d) in ^{208}Pb. The numbers given in the ordinates and abscissas refer to the order of parameters defined in Ref. [7], that is, ρ_c, E^{NM}/A, a_{sym}^{NM}, L_{sym}^{NM}, $C_0^{\rho\Delta\rho}$, $C_1^{\rho\Delta\rho}$, V_0^n, V_0^p, $C_0^{\rho\nabla J}$, and $C_1^{\rho\nabla J}$.

In Table I, we listed the s.p. energies and their standard errors calculated in ^{208}Pb. We see that the proton (neutron) rms of standard errors, equal to 0.196 (0.176) MeV, is significantly smaller than the rms deviations with respect to empirical data [25] of 0.52 (0.61) MeV. The rms deviations obtained in lead are still much smaller than those obtained when all doubly-magic nuclei are considered simultaneously, which typically equal to about 1.2 MeV [26], quite independently of which functional and which data evaluation is used. Anyhow, we see again that the s.p. energies, which in the fit of the UNEDF0 functional were not taken into account, are rather tightly constrained by the fit to other observables. It is, therefore, unlikely that, within the parameter space of the standard Skyrme functional, their agreement with data can be improved, which supports conclusions reached in Ref. [26].

Of course, in principle, the obtained insufficient agreement with data can also signal some important missing physics. For the s.p. energies, an obvious and often invoked effect is the well-known particle-vibration-coupling (PVC) [27], which continues to be the subject of recent works [28–30]. Before studying this problem for the Skyrme functionals in full detail [31], in Table I we presented the PVC corrections to s.p. energies, δe_{PVC}, calculated with the standard methodology reviewed recently in, e.g., Ref. [29]. We see that in the particular case studied here, the inclusion of the PVCs does not improve the agreement with data, but, in fact, the rms deviation obtained for protons (neutrons) even increases to 0.70 (0.68) MeV. An improved agreement with data should probably be sought for by using richer parameter spaces of the functional, such as, e.g., those proposed in Refs. [5, 32]. Evidently, further studies of this problem are very much required.

TABLE I: The ^{208}Pb proton (top) and neutron (bottom) s.p. energies e_{HF} (b) and their standard errors (c), as compared to the empirical values (d) [25], residuals, $\Delta(e_{HF}) = e_{HF} - e_{exp}$ (e), PVCs δe_{PVC} (f), and residuals of the PVC-corrected s.p. energies $\Delta(e_{PVC}) = e_{HF} + \delta e_{PVC} - e_{exp}$ (g). Where applicable, we also give the root-mean-square (rms) values of entries shown in a given column. All energies are in MeV.

orbital	e_{HF}	$\sigma(e_{HF})$	e_{exp}	$\Delta(e_{HF})$	δe_{PVC}	$\Delta(e_{PVC})$
(a)	(b)	(c)	(d)	(e)	(f)	(g)
$\pi 3p_{1/2}$	0.219	0.181	−0.16	0.38	−0.440	−0.06
$\pi 3p_{3/2}$	−1.045	0.139	−0.68	−0.37	−0.662	−1.03
$\pi 2f_{5/2}$	−1.284	0.229	−0.97	−0.31	−0.480	−0.79
$\pi 1i_{13/2}$	−2.794	0.238	−2.10	−0.69	−0.221	−0.92
$\pi 1h_{9/2}$	−3.501	0.282	−3.80	0.30	−0.280	0.02
$\pi 2f_{7/2}$	−3.725	0.115	−2.90	−0.83	−0.284	−1.11
$\pi 3s_{1/2}$	−8.036	0.140	−8.01	−0.03	−0.108	−0.13
$\pi 2d_{3/2}$	−8.378	0.199	−8.36	−0.02	0.220	0.20
$\pi 1h_{11/2}$	−9.153	0.207	−9.36	0.21	−0.141	0.07
$\pi 2d_{5/2}$	−10.117	0.117	−9.82	−0.30	0.116	−0.18
$\pi 1g_{7/2}$	−10.908	0.229	−12.00	1.09	0.131	1.22
rms	n.a.	0.196	n.a.	0.52	0.328	0.70
$\nu 3d_{3/2}$	−1.856	0.250	−1.40	−0.46	−0.104	−0.56
$\nu 4s_{1/2}$	−2.051	0.235	−1.90	−0.15	−0.668	−0.82
$\nu 2g_{7/2}$	−2.141	0.258	−1.44	−0.70	−0.280	−0.98
$\nu 1f_{15/2}$	−2.231	0.167	−2.51	0.28	−0.226	0.05
$\nu 3d_{5/2}$	−2.549	0.166	−2.37	−0.18	−0.384	−0.56
$\nu 1i_{11/2}$	−2.680	0.223	−3.16	0.48	−0.271	0.21
$\nu 2g_{9/2}$	−4.336	0.071	−3.94	−0.40	−0.183	−0.58
$\nu 3p_{1/2}$	−7.855	0.109	−7.37	−0.49	0.152	−0.33
$\nu 3p_{3/2}$	−8.503	0.065	−8.26	−0.24	−0.119	−0.36
$\nu 2f_{5/2}$	−8.519	0.143	−7.94	−0.58	0.156	−0.42
$\nu 1i_{13/2}$	−8.603	0.162	−9.24	0.64	−0.130	0.51
$\nu 1h_{9/2}$	−9.922	0.190	−11.40	1.48	0.120	1.60
$\nu 2f_{7/2}$	−10.407	0.103	−9.81	−0.60	0.179	−0.42
rms	n.a.	0.176	n.a.	0.61	0.273	0.68

Summary and Conclusions. In the framework of the UNEDF0 Skyrme-EDF model, we studied propagation of uncertainties from model parameters to calculated observables. We found that the magnitude of standard errors increases towards neutron rich nuclei. This is directly linked to the isovector part of the functional, where coupling constants have large uncertainties.

For binding energies, the standard errors are in the range of one to several MeV – towards the neutron drip line rapidly increasing to about 10 Mev. For two-particle separation energies, they range from a few hundred keV to a few MeV. Compared to the deviations from experimental values, the standard errors of binding energies are, in the experimentally known region, of the same order of magnitude or somewhat smaller. For two-particle sepa-

ration energy, standard errors are typically smaller, but still comparable. It is worth stressing that the theoretical uncertainties of binding energies and two-particle separation energies are still much larger than the present experimental errors in Penning-trap measurements [33, 34]. For proton rms radii, our standard errors are also comparable, but slightly smaller than the rms deviations from experimental values. Theoretical uncertainties related to the neutron skin are actually smaller than the current experimental estimates [18].

In conclusion, determination of theoretical uncertainties in terms of standard statistical errors of observables provides a way to assess the predictive power of nuclear models. In the future EDF parameter optimizations, it would be useful to perform by default the sensitivity analyses of the obtained minima. With this information, theoretical uncertainties related to the model parameters and predictions should be routinely assessed.

Acknowledgments. Interesting comments by Witek Nazarewicz are gratefully acknowledged. We thank Gillis Carlsson for his help with upgrading the numerical code. This work was supported in part by the Academy of Finland and University of Jyväskylä within the FIDIPRO programme, by the Centre of Excellence Programme 2012–2017 (Nuclear and Accelerator Based Physics Programme at JYFL), and by the European Union's Seventh Framework Programme ENSAR (THEXO) under Grant No. 262010. We acknowledge the CSC - IT Center for Science Ltd, Finland, for the allocation of computational resources.

[1] J. Toivanen, J. Dobaczewski, M. Kortelainen, and K. Mizuyama, Phys. Rev. C **78**, 034306 (2008).
[2] J. Dudek, B. Szpak, M.-G. Porquet, H. Molique, K. Rybak, and B. Fornal, J. Phys. G **37**, 064031 (2010).
[3] P.-G. Reinhard and W. Nazarewicz, Phys. Rev. C **81**, 051303 (2010).
[4] J. Erler, N. Birge, M. Kortelainen, W. Nazarewicz, E. Olsen, A. M. Perhac, and M. Stoitsov, Nature **486**, 509 (2012).
[5] J. Dobaczewski, K. Bennaceur, and F. Raimondi, J. Phys. G **39**, 125103 (2012).
[6] P. Klüpfel, P.-G. Reinhard, T.J. Burvenich, and J.A. Maruhn, Phys. Rev. C **79**, 034310 (2009).
[7] M. Kortelainen, T. Lesinski, J. Moré, W. Nazarewicz, J. Sarich, N. Schunck, M.V. Stoitsov, and S. Wild, Phys. Rev. C **82**, 024313 (2010).
[8] F.J. Fattoyev and J. Piekarewicz, Phys. Rev. C **84**, 064302 (2011).
[9] M. Kortelainen, J. McDonnell, W. Nazarewicz, P.-G. Reinhard, J. Sarich, N. Schunck, M.V. Stoitsov, and S. Wild, Phys. Rev. C **85**, 024304 (2012).
[10] J. Piekarewicz, B.K. Agrawal, G. Colò, W. Nazarewicz, N. Paar, P.-G. Reinhard, X. Roca-Maza, and D. Vretenar, Phys. Rev. C **85**, 041302(R) (2012).
[11] M. Bender, P.-H. Heenen, and P.-G. Reinhard, Rev. Mod. Phys. **75**, 121 (2003).
[12] F.J. Fattoyev and J. Piekarewicz, Phys. Rev. C **86**, 015802 (2012).
[13] P.-G. Reinhard and W. Nazarewicz, Phys. Rev. C **87**, 014324 (2013).
[14] L.F. Richardson and J.A. Gaunt, Phil. Trans. R. Soc. Lond. A **226** 299 (1927).
[15] B.G. Carlsson, J. Dobaczewski, J. Toivanen, and P. Veselý, Comput. Phys. Commun. **181**, 1641 (2010).
[16] B.G. Carlsson, J. Toivanen, P. Veselý, and Y. Gao, *unpublished*.
[17] M.V. Stoitsov, J. Dobaczewski, W. Nazarewicz, S. Pittel, and D.J. Dean, Phys. Rev. C **68**, 054312 (2003).
[18] M. Kortelainen, J. Erler, N. Birge, Y. Gao, W. Nazarewicz, and E. Olsen, *unpublished*.
[19] G. Audi, F.G. Kondev, M. Wang, B. Pfeiffer, X. Sun, J. Blachot, and M.MacCormick, Chinese Physics **C36**, 1157 (2012); G. Audi, M. Wang, A.H. Wapstra, F.G. Kondev, M. MacCormick, X. Xu, and B. Pfeiffer, Chinese Physics **C36**, 1287 (2012); M. Wang, G. Audi, A.H. Wapstra, F.G. Kondev, M. MacCormick, X. Xu, and B. Pfeiffer, Chinese Physics **C36**, 1603 (2012).
[20] M. Bender, G. Bertsch, and P.-H. Heenen, Phys. Rev. C **73**, 034322 (2006).
[21] J.-P. Delaroche, M. Girod, J. Libert, H. Goutte, S. Hilaire, S. Péru, N. Pillet, and G.F. Bertsch, Phys. Rev. C **81**, 014303 (2010).
[22] B.G. Carlsson, J. Toivanen, and U. von Barth, arXiv:1212.2050.
[23] C.J. Horowitz, Z. Ahmed, C.-M. Jen, A. Rakhman, P.A. Souder, M.M. Dalton, N. Liyanage, K.D. Paschke, K. Saenboonruang, R. Silwal, G.B. Franklin, M. Friend, B. Quinn, K.S. Kumar, D. McNulty, L. Mercado, S. Riordan, J. Wexler, R.W. Michaels, and G.M. Urciuoli, Phys. Rev. C **85**, 032501 (2012).
[24] S. Abrahamyan, Z. Ahmed, H. Albataineh, *et. al.*, Phys. Rev. Lett. **108**, 112502 (2012).
[25] N. Schwierz, I. Wiedenhover, and A. Volya, arXiv:0709.3525.
[26] M. Kortelainen, J. Dobaczewski, K. Mizuyama, and J. Toivanen, Phys. Rev. C **77**, 064307 (2008).
[27] A. Bohr and B.R. Mottelson, *Nuclear Structure* (Benjamin, New York, 1975), Vol. II.
[28] E. Litvinova, P. Ring, and V. Tselyaev, Phys. Rev. C **75**, 064308 (2007).
[29] G. Colò, H. Sagawa, and P.-F. Bortignon, Phys. Rev. C **82**, 064307 (2010).
[30] K. Mizuyama, G. Colò, and E. Vigezzi, Phys. Rev. C **86**, 034318 (2012).
[31] D. Tarpanov *et al.*, unpublished.
[32] B.G. Carlsson, J. Dobaczewski, and M. Kortelainen, Phys. Rev. C **78**, 044326 (2008); **81**, 029904(E) (2010).
[33] J. Hakala, J. Dobaczewski, D. Gorelov, T. Eronen, A. Jokinen, A. Kankainen, V.S. Kolhinen, M. Kortelainen, I.D. Moore, H. Penttilä, S. Rinta-Antila, J. Rissanen, A. Saastamoinen, V. Sonnenschein, and J. Äystö, Phys. Rev. Lett. **109**, 032501 (2012).
[34] A. Kankainen, J. Äystö, and A. Jokinen, J. Phys. G **39**, 093101 (2012).